

Acoustical resonances of assorted ancient structures

Robert G. Jahn

*Princeton Engineering Anomalies Research, School of Engineering and Applied Science,
Princeton University, Princeton, New Jersey 08544-5263*

Paul Devereux

39 Alma Place, Penzance TR18 2BX, United Kingdom

Michael Ibison

*Princeton Engineering Anomalies Research, School of Engineering and Applied Science,
Princeton University, Princeton, New Jersey 08544-5263*

(Received 8 June 1995; revised 30 October 1995; accepted 30 November 1995)

Rudimentary acoustical measurements performed inside six diverse ancient structures revealed that each sustained a strong resonance at a frequency between 95 and 120 Hz, despite major differences in chamber shapes and sizes. The resonant modal patterns all featured strong antinodes at the outer walls, with appropriately configured nodes and antinodes interspersed toward the central source. In some cases, interior and exterior rock drawings resembled these acoustical patterns. Since the resonance frequencies are well within the adult male voice range, one may speculate that some forms of human chanting, enhanced by the cavity resonance, were invoked for ritual purposes. © 1996 Acoustical Society of America.

PACS numbers: 43.10.Ln, 43.55.Gx, 43.55.Br, 43.20.Ks

INTRODUCTION

On an earlier informal tour of certain Anazasi sites in the US Southwest, the authors were struck by the acoustical resonances of various kivas and other ceremonial facilities, and mused whether similar properties might prevail in the more primitive neolithic structures that abound in the United Kingdom. To assess such possibilities empirically, a modest itinerary, rudimentary equipment package, and simple protocol were assembled to constitute a pilot experiment that was carried out over a 10-day period in mid-July 1994. The sites visited are detailed in Table I. (No quantitative measurements were taken at the Anazasi sites, and we are unaware of any reports in the literature. We are considering extension of the studies reported to those environments.)

Experimental design

The equipment deployed consisted of an omnidirectional loudspeaker (Realistic #40-1352) driven by a variable frequency sine-wave oscillator (Bruel & Kjaer Precision, #3026) and a 20-W amplifier (Radio Shack MPA-30, #32-2034), with sound frequency verified by an external, hand-held digital multimeter (Extech TMT-3885, #3802285). The sound amplitude patterns were mapped by a portable meter (Realistic #33-2050), sensitive between 55 and 105 dB sound-pressure level. In a typical experiment, the source was placed on the floor or on a short tripod roughly at the center of the chamber configuration, with the acoustic axis oriented vertically. (While it is clear that such placement preferentially excites angularly symmetric modes, most of the sites left little option for placement elsewhere.) The frequency was manually swept through the lower audible range until the lowest natural resonance of the cavity was evidenced by clearly discernible reverberation of the chamber. With this

established, the sound intensity was adjusted to the highest comfortable level, usually between 100 and 110 dB at the source, and horizontal surveys of standing-wave patterns were made over some accessible grid covering the chamber. In some cases, vertical or inclined profiles were also attempted.

To varying degrees, the completeness and precision of these surveys were severely constrained by the limited times available at the sites, intrusion of tourists, awkwardness of the spaces, and control agency requirements, so that only rudimentary maps could be obtained by the experimenters crawling about the cavities. (It is acknowledged that the presence of the experimenters in the chambers will slightly increase the frequency of the resonances and the damping, but this would also have been a feature of their use in antiquity.) Notwithstanding these difficulties, certain features were clearly established:

(1) Characteristic resonance frequencies of the various sites were well defined. After very little practice, the experimenters could blind-tune the source frequency to a clearly audible resonance with a reproducibility of ± 1 or 2 Hz with little ambiguity.

(2) Although many shapes and sizes of chamber were presented, the dominant resonance frequencies of all of them lay in the range between 95 and 120 Hz.

(3) In all cases, principal antinodes of resonant standing-wave patterns were established at the outer walls, as would be expected theoretically. The number, configuration, and relative magnitudes of the other antinodes and nodes leading back to the source depended on the particular chamber configuration.

(4) In some cases, rock art on the chamber walls bore some similarity to the observed standing-wave patterns.

TABLE I. Ancient sites studied.

Site	Location	Age	Configuration
Wayland's Smithy	Berkshire, UK	ca. 3500 BC	5-m cruciform chamber inside 55×15-m trapezoidal mound.
Chun Quoit	Cornwall, UK	ca. 3500 BC	1.5×1.5×1.7-m trapezoidal chamber under 3×3-m capstone.
Cairn Euny	Cornwall, UK	ca. 400 BC	"Beehive" chamber 5 m diam×2.5 m high.
Cairn L.	Loughcrew,	ca. 3500 BC	Irregular array of central chamber, seven sub-chambers, and passage, 6×5×3 m, inside 130-m-diam mound.
Carnbane West	Co. Meath, Ireland		
Cairn I.	Loughcrew,	ca. 3500 BC	Roughly elliptical array of seven sub-chambers, central chamber, and passage, 4×3.5 m overall, originally inside 55-m-diam mound.
Carnbane West	Co. Meath, Ireland		
Newgrange	Co. Meath, Ireland	ca. 3500 BC	6.5×6.5-m cruciform chamber reached by 19-m passage, inside 50-m-diam mound.

I. SPECIFIC RESULTS

A. Wayland's Smithy, Berkshire, United Kingdom

This cruciform chamber, ca. 3500 BC, lies within a 43-m-long trapezoidal mound. Each of its sub-chambers is roughly 1.5×1.5×1.0-m interior size, as is its entrance passage. A 1919 excavation revealed 8 skeletons, including one child. The name of this site derives from folk legend that predicts that if a horse and a piece of silver are left overnight, the spectral "Wayland the Smith" will shoe the animal. Acoustical mapping of this complex suffered from its cramped configuration and our early inexperience with the field equipment and mapping strategies. As shown in Fig. 1, the source was placed on the floor at the center of the cross, and radial surveys were made into the east and west chambers only. The former, which was the more thoroughly mapped, resonated most strongly at 112 Hz, at which frequency it displayed standing-wave antinodes at its entrance

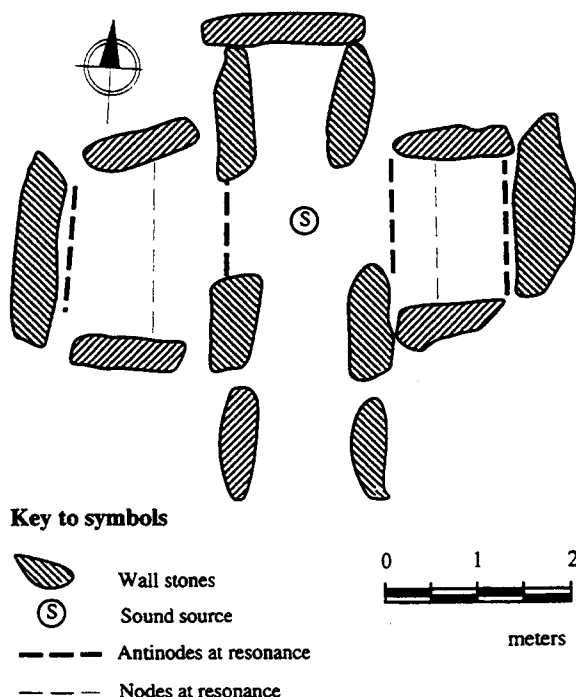


FIG. 1. Wayland's Smithy—plan view of modal pattern.

orifice and at its far wall, separated by one intermediate node. A secondary resonance was identified at 119 Hz, which featured a third antinode roughly one-third of the way into the chamber, separated from the others by two interior nodes. The west chamber, which was less thoroughly mapped, appeared to resonate more strongly at 95 Hz, producing a double antinode pattern akin to that in the east chamber at 112 Hz. The north, central, and entrance chambers were not mapped. (More detailed descriptions and photographs of sites, reports and analyses of results are available in Jahn *et al.*, 1995.)

B. Chun Quoit, Cornwall, United Kingdom

This stone chamber or dolmen, ca. 3500 BC, consisting of four inward-leaning slabs supporting a capstone weighing several tons, is roughly 1.5×1.5 m at its base and 1.7 m high, and was originally surrounded by a cairn of stone. It is speculated that such dolmens were used as ritual burial sites, and for oracular purposes. Again, because of the limited interior space, only a rudimentary survey could be made, and that only with the source placed near the front wall (Fig. 2). A composite resonance frequency of 110 Hz was identified, with antinodes located at the source and at the far wall, with one node midway between. A vertical survey at the node position revealed a positive intensity gradient up to the ceiling, and some further reinforcement of amplitudes at the interior corners was also observed. The huge capstone of this structure had interesting acoustical properties of its own. When struck with a hard object, it reverberated with an assortment of modes based on a major fifth chord interval above the chamber resonant frequency.

C. Cairn Euny, Cornwall, United Kingdom

This corbelled "beehive" chamber is attached to a fogou (underground passage) beneath an Iron Age village, ca. 400 BC. The original roof has now been partially capped by metal sheeting. A small recess, of unknown purposes, faces the short entrance passage. The chamber diameter is roughly 5 m, and its central height about 2.5 m. With the source placed on a short tripod at the center, this structure resonated at 99 Hz, establishing the concentric modal pattern sketched in Fig. 3, with a single node at a radius of about 1.7 m. The

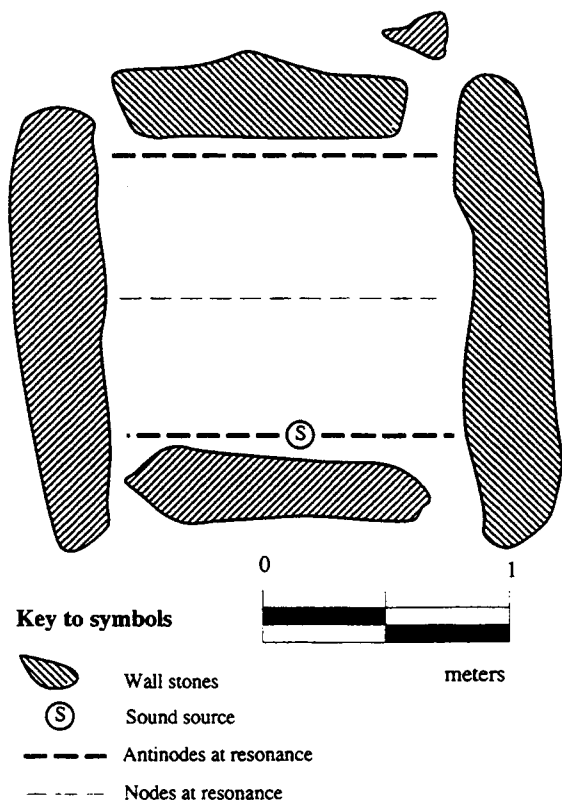


FIG. 2. Chun Quoit—plan view of modal pattern.

pattern was azimuthally quite uniform, with the exception of the regions near the entrance passage and the opposite recess.

D. Cairn L, Carnbane West, Loughcrew, Ireland

This is one of several chambered stone cairns, ca. 3500 BC, usually described as “passage tombs,” that are scattered about a ridge of the Loughcrew Hills known locally as “Hill of the Witch.” The entire cairn is 135 m in circumference, but its irregularly shaped inner chamber is only about 6×5 m, and 3 m high. Its 5-m-long entrance passage is oriented toward the southeast, allowing sunrise light to fall on an interior free-standing limestone pillar on particular days of the year. The chamber is sectored into seven sub-chambers by appropriately placed standing stones. One of these sub-chambers contains an exceptional basin and backstone, and some of its walls display exquisitely carved patterns. With the source on a short tripod at the center of the main chamber, eight radial surveys were taken in the horizontal plane of the source, penetrating into each of the sub-chambers and the entrance passage. The overall plan view of the modal pattern at the dominant resonance frequency of 110 Hz is sketched in Fig. 4. Each of the shorter sub-chambers sustained a single antinode at the wall, with its associated node slightly inside the chamber orifice. The one deeper chamber directly opposite the entrance passage displayed two antinodes and two nodes, as sketched. Unfortunately, the pattern along the passage was not mapped much beyond its interior orifice. Vertical traverses up the back walls of the large sub-chamber

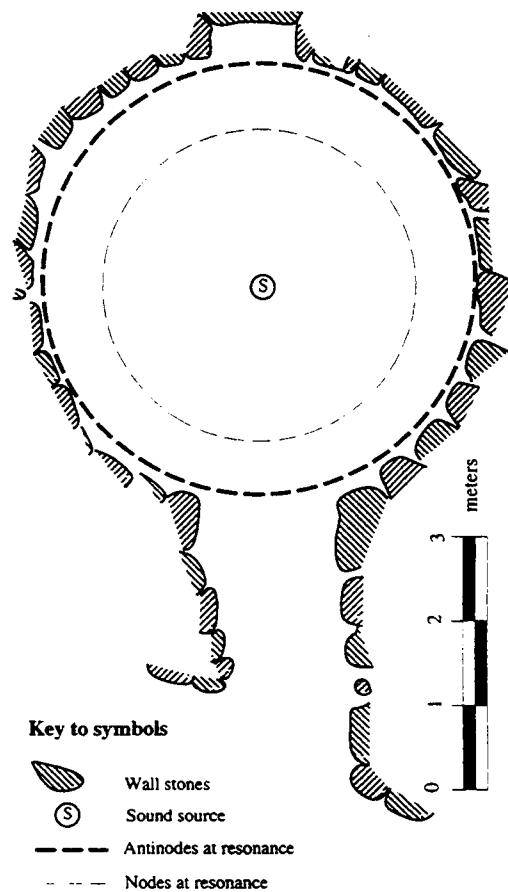


FIG. 3. Cairn Euny—plan view of modal pattern.

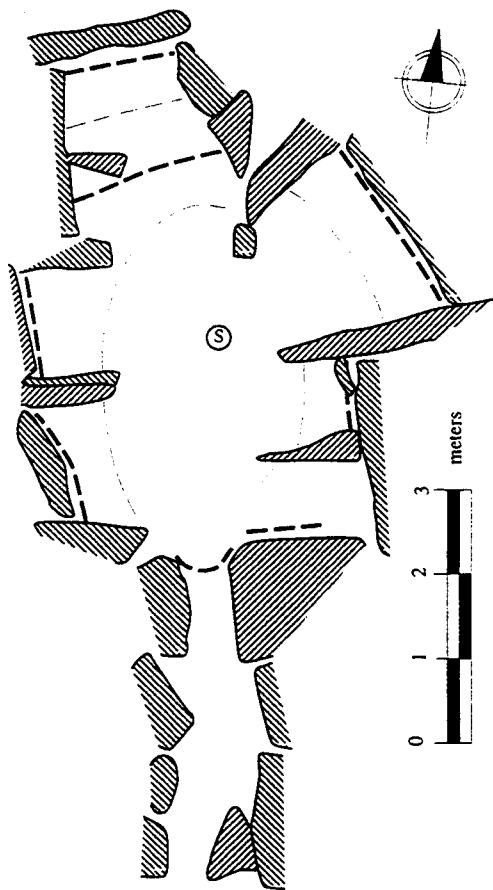
and the basin sub-chamber were unremarkable. (Detailed graphs of all of the radial traverses of this and the other sites are presented in Jahn *et al.*, 1995.)

E. Cairn I, Carnbane West, Loughcrew, Ireland

This satellite cairn lies a few hundred yards southwest of Cairn L and is of similar configuration to it, albeit smaller in scale, and now roofless. The encompassing mound is about 55 m in diameter, and the overall chamber configuration roughly 4 m in major axis. Again there are seven sub-chambers and excellent wall carvings. Eight radial profiles were mapped outward from the source, with results similar to Cairn L. In this case, all sub-chambers sustained only one antinode at the outer walls, and one interior node (Fig. 5). For the three shorter sub-chambers farthest from the entrance, the nodes formed in the central chamber rather than inside the cells, but otherwise the overall plan pattern closely resembled that of Cairn L.

F. Newgrange, County Meath, Ireland

The most impressive of all sites surveyed was this 5500-years-old cairn near the Boyne River [Fig. 6(a)]. It features a remarkable 19-m-long entrance passage, again opening to the southeast and floridly decorated with rock art, leading to a 6.5×6.5-m cruciform configuration composed of a central



Key to symbols





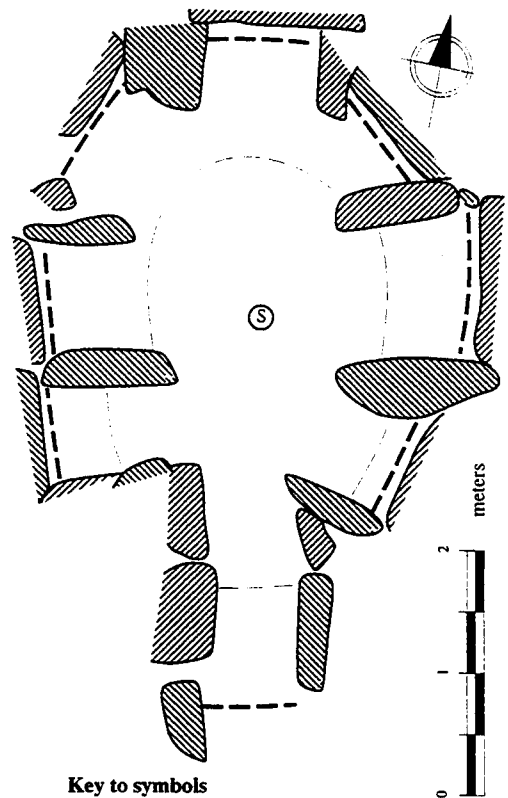
-  Wall stones
-  Sound source
-  Antinodes at resonance
-  Nodes at resonance

FIG. 4. Louchcrew Cairn L—plan view of modal pattern.



Key to symbols





-  Wall stones
-  Sound source
-  Antinodes at resonance
-  Nodes at resonance

FIG. 5. Louchcrew Cairn I—plan view of modal pattern.

chamber and three sub-chambers. Each of the sub-chambers contain a mysterious stone basin, and further magnificent rock art designs. With the sound source at its center on a short tripod, the chamber complex resonated at 110 Hz, at which the standing-wave patterns sketched in Figs. 6(b), 6(c), and 6(d) were established. Radial traverses into the two shorter sub-chambers each showed two nodes and two antinodes, one at the outer wall, and one near the sub-chamber orifice. The deepest sub-chamber allowed a third node-antinode pair to stand inside itself. The overall plan pattern thus involved a closed node in the central chamber, and a closed antinode near the sub-chamber and passage orifices, progressing into the sub-chamber patterns just mentioned. Equally if not more remarkable was the pattern of standing waves sustained along the entire length of the entrance passage. Despite its comparatively small cross section (roughly 1 m wide \times 2 m high), and the large- and small-scale irregularities of the stones forming its walls and ceiling, some 12 antinode/node pairs could be clearly discerned, extending over its full length from chamber to outside entrance in a

classic sinusoidal pattern akin to that of some gigantic wind instrument [Fig. 6(d)].

II. THEORETICAL PREDICTIONS

In principle, it should be possible to calculate analytically the permitted modal patterns and associated resonance frequencies directly from the known chamber configurations and dimensions. In practice, however, due to major irregularities that now prevail in the various interior surfaces, and also because analytical solutions in terms of standard functions are possible only for the simplest of geometries, such a comprehensive approach is doomed to complex numerical simulations. A less ambitious strategy would be to idealize the site geometries to permit analytical searches for self-consistent patterns between adjacent sub-chambers (cf. the partitioning method described below), but even here, the plethora of possible modalities precludes specification of unique solutions without resorting to some empirical data. Thus, more practical for our purposes is simply to allow the experimental observations to indicate the particular modalities to be considered, and for these to calculate the expected standing-wave patterns and frequencies for comparison with the data. Here we outline the results of a few such attempts

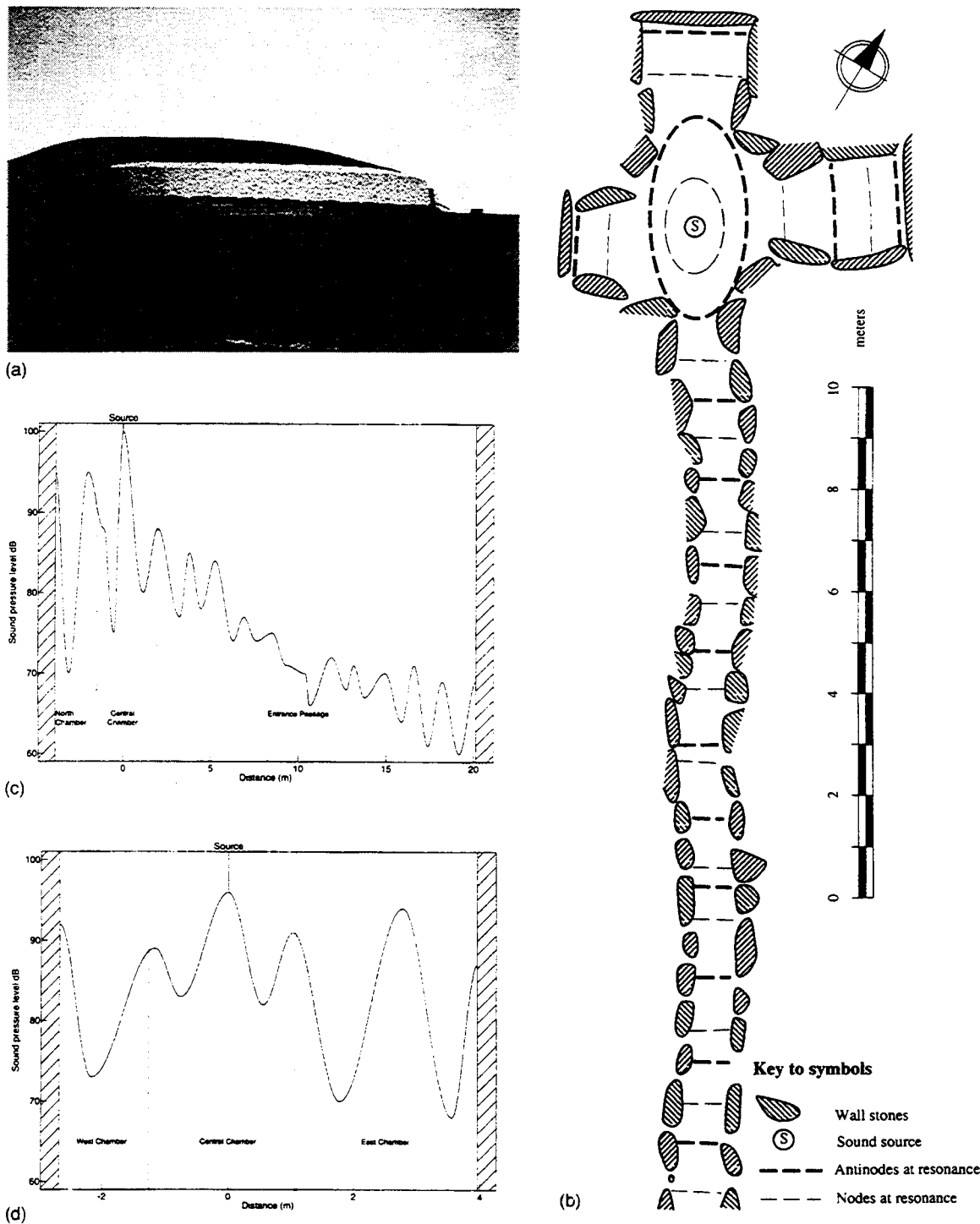


FIG. 6. (a) New Grange—photograph of site; (b) New Grange—plan view of modal pattern; (c) New Grange—long axis traverse; (d) New Grange—short axis traverse.

for the various sites, now presented in order of increasing complexity. Further details of these calculations are presented in Jahn *et al.*, 1995.

A. General approach

We denote by ω_m the resonance frequencies corresponding to solutions of the reduced wave equation for the acoustic potential. Where Cartesian coordinates are used, x denotes the longitudinal dimension in the horizontal plane (i.e.,

in the direction normal to the opening of the chamber under discussion). Coordinates y and z denote the perpendicular horizontal and vertical directions, respectively. The dimensions of cuboidal (rectangular parallelepiped) chambers are correspondingly denoted by l_x , l_y , and l_z . For these calculations, we assume perfect reflection at the stone walls and at any major openings to the outside. Interior obstacles much smaller than the resonant wavelengths are neglected. The speed of sound is taken to be 344 m/s throughout.

Application of this formalism to our particular structures requires a few other ad hoc strategies appropriate to individual situations, as detailed below. In all cases, however, our attention focuses on the lowest frequency members of the theoretically possible resonances, since these are found to be relatively pronounced and of similar frequencies across the sites, compared to the distribution of higher resonances within the sites. We also note that these lower frequencies are more accessible to the male human acoustical generation and detection physiology. The human male voice can generate a relatively high intensity in this range, and the human ear can detect it sensitively and comfortably, even though it is not a range that contributes to speech intelligibility to any significant extent.

B. Chun Quoit

The inward slanting walls and slightly tipped ceiling of this dolmen present an interior volume that is trapezoidal in its three cross sections and is further complicated by stone surface irregularities and the entrance aperture at one corner. For purposes of crude comparison with theory, we idealize the space as a cuboid, 1.5 m × 1.5 m in horizontal cross section and 1.7 m high. We denote by $\{n_x, n_y, n_z\}$ the rectilinear modes corresponding to the number of half-wavelengths contained between the walls. Because of the difficulty of maneuvering the sound detector around this space without obstructing the source, the latter had to be placed on the floor adjacent to the front wall ($x=0, y=l_y/2, z=0$). Consistent with this placement, the sound patterns mapped showed clearly antinodes at the front and back walls ($x=0$ and $x=l_x$), and a node at the center ($x=l_x/2$), as sketched in Fig. 2(b). Traverses in the y and z directions, although showing some variations, were more ambiguous, suggesting that the dominant mode was $\{1,0,0\}$. Using

$$\omega_{\mathbf{m}} = \pi c \sqrt{\frac{n_x^2}{l_x^2} + \frac{n_y^2}{l_y^2} + \frac{n_z^2}{l_z^2}}, \quad (1)$$

and denoting the theoretically computed modes by $\{n_x, n_y, n_z; \omega_{\mathbf{m}}/2\pi\}$, we find that the three modes $\{0,0,1;103\}$, $\{1,0,0;113\}$, and $\{0,1,0;113\}$ are virtually indistinguishable in frequency, with the next closest in frequency well removed at 152 Hz. For an isotropic source, there would be no *a priori* reason to select any one of these modes in preference to the others, and some combination of them could contribute to the lowest perceived resonance. But given the little nodality observed in the vertical direction, along with the necessary placement of the source near the entrance wall, it appears that $\{1,0,0;113\}$ dominates, in good agreement with the measured frequency of 110 Hz.

C. Louchcrew I

The simplest idealization that suggests itself for this uncovered structure is to treat it as a vertical elliptical cylinder, closed on the bottom and open on top, sectorized by eight standing stone partitions. The entrance passage can be expected to distort the elliptical phase fronts somewhat, although the opening is a relatively small fraction of the boundary seen by an elliptical mode and may be neglected

when considering modes with little or no variability in the angular direction. The radially oriented stones form open sub-chambers around the central chamber of the structure, but because these stones are narrow, each subtends a relatively small angle and again may be neglected for modes with little or no variability in the angular direction. (It is tempting to speculate whether the builders purposely aligned the sector stones to yield a sharper resonance.)

Separating the acoustical wave equation in elliptical-cylindrical coordinates yields standing-wave solutions in the form of Mathieu functions, which we index by $\{l, m, n\}$ corresponding to the radial, azimuthal, and vertical quantum numbers. Given the absence of any clear azimuthal or vertical structure in the measured patterns, we may again focus on modes with only radial variation. It should also be noted that the current absence of a ceiling of the chamber distorts the vertical profile as now measured from what would have prevailed in the closed configuration, but even then, given the modest chamber height, it is unlikely that any modes having major vertical variation would have been significant contributors to the pattern at low frequencies. The modality is further constrained by the appearance of only one node in the measured radial traverses [Fig. 5(b)], indicating that $\{1,0,0\}$ is the dominant pattern. In somewhat more detail, we label the coordinates of the elliptical cylinder $\mathbf{r} \equiv \{\xi, \zeta, z\}$, where ξ, ζ are, respectively, the “elliptical radius” and “elliptical angle” and z is the vertical direction, and we denote the mode index by $\mathbf{m} \equiv \{l, m, n\}$. The full solution for the acoustic potential is then (McLachlan, 1964):

$$\begin{aligned} \phi = & \sum_{l=0}^{\infty} \sum_{m=0}^{\infty} \sum_{n=0}^{\infty} a_{l,m,n}^{(+)} Ce_m(\xi, q_{m,l}^{(+)}) ce_m(\zeta, q_{m,l}^{(+)}) \\ & \times \cos(n\pi z/l_z) \cos(\omega_{l,m,n}^{(+)} t) \\ & + \sum_{l=0}^{\infty} \sum_{m=1}^{\infty} \sum_{n=0}^{\infty} a_{l,m,n}^{(-)} Se_m(\xi, q_{m,l}^{(-)}) se_m(\zeta, q_{m,l}^{(-)}) \\ & \times \cos(n\omega z/l_z) \cos(\omega_{l,m,n}^{(-)} t). \end{aligned} \quad (2)$$

The ce and se are Mathieu functions of the first kind, the Ce and Se are modified Mathieu functions of the first kind (McLachlan, 1964; Abramowitz and Stegun, 1970). The superscripts (+) and (−) indicate symmetry about the major and minor axes, respectively. The special case $m=0$, although associated with the (+) label, corresponds to modes with no angular variation, and are therefore trivially symmetric about both major and minor axes. The eigenvalues $q_{m,l}^{(\pm)}$ are determined by the boundary conditions

$$Ce'_m(\xi_0, q_{m,l}^{(+)}) = 0, \quad Se'_m(\xi_0, q_{m,l}^{(-)}) = 0, \quad (3)$$

where

$$\xi_0 \equiv \cosh^{-1}(1/e), \quad e \equiv \sqrt{1 - b^2/a^2} \quad (4)$$

are, respectively, the “elliptical radius” to the walls from the nominal origin and the eccentricity of the ellipse. Here a and b are the semi-major and semi-minor axes. The corresponding resonance frequencies are

$$\omega_{l,m,n}^{(\pm)} = c \sqrt{\frac{4q_{m,l}^{(\pm)}}{a^2 - b^2} + \frac{n^2 \pi^2}{l_z^2}} \quad (5)$$

Although Loughcrew I is now roofless, there are indications that a roof existed at around 2.0-m height. Using this and other measured dimensions, we take $a=2.5$ m, $b=1.8$ m, and $l_z=2.0$ m, whence Eq. (4) gives $e=0.69$ and $\xi_0=0.91$. The measured resonant $\{1,0,0\}$ mode has no angular or vertical variation, so we solve numerically for $q_{0,1}^{(+)}$ from the boundary conditions in Eq. (3) to find that $q_{0,1}^{(+)}=2.8$. Inserting this and the dimensions above into Eq. (5) gives a resonance frequency of 106 Hz, in good agreement with the observed frequency of 112 Hz. This mode has an antinode at the source and at the walls, and a single node whose location is found from the condition $Ce_0(\xi, q_{0,1}^{(+)}) = 0$ to be at $\xi=0.5$. To compare this prediction with the measured location of the node as it intersects the major axis ($y=0, \zeta=0$) we use the relation $x=ae \cosh(\xi) \cos(\zeta)$, which gives $x=1.9$ m as the intersect. The measured resonance at 112 Hz was found to have a node surface ranging from 1.25–2.15 m from the source, giving 1.7 m as the symmetrized intersect with the major axis. These results are well within the tolerances, notwithstanding our neglect of the radially oriented stones.

D. Cairn Euny

We approximate the structure of Cairn Euny as a hemisphere of radius 2.5 m. Separability demands that the wave equation be written in cylindrical polars $\mathbf{r} \equiv \{r, \theta, \phi\}$, corresponding to the radius, the angle in the horizontal plane, and the polar angle, respectively (not to be confused with the acoustic potential). In a closed sphere the modes are products of spherical harmonics and modified Bessel functions of the radius (Schiff, 1968). In a hemisphere the situation is more complicated, but can be simplified if attention is restricted in advance, in accord with measurements, to modes with no angular variation in the horizontal plane at the base of the structure. Denoting the radial, horizontal angle, and azimuthal quantum numbers by $\mathbf{m} \equiv \{l, m, n\}$, with $m=0$, gives

$$\phi = \sum_{l=0}^{\infty} \sum_{n=0}^{\infty} a_{l,n} j_n(u_{n,l} r/a) P_n(\cos(\phi)) \cos(\omega_{l,n} t), \quad (6)$$

where the j_n are spherical Bessel functions of order n (Abramowitz and Stegun, 1970) and the P_n are Legendre functions (Abramowitz and Stegun, 1970) The $u_{n,l}$ are determined by the boundary condition at $r=a$,

$$j_n'(u_{n,l}) = 0, \quad (7)$$

and the boundary condition at the base of the structure requires n to be even. The corresponding resonance frequencies are

$$\omega_{l,n} = c u_{n,l} / a. \quad (8)$$

The eigenvalues $u_{n,l}$ solving Eq. (7) are tabulated, for instance in (Abramowitz and Stegun, 1970). Using $a=2.5$, computation of the resonances from Eq. (8) reveals that the mode $\{1,0,0;99\}$ has the lowest frequency (given the empirical observation that there is no angular variation in the base plane). This is in exact agreement with the measured reso-

nance and correctly predicts the measured modal pattern. In particular, the node in the base plane is predicted to be at a radius r given by the first zero of $j_0(u_{0,0} r/a)$, which occurs at $u_{0,0} r/a = \pi$. Determining from Eq. (7) that $u_{0,0}=4.5$ gives $r=1.75$ m, in close agreement with the measured value.

E. Loughcrew L

To obtain a rough initial estimate of the resonances of this composite covered chamber, we model the whole structure as an ellipsoidal cylinder. Using a semi-major axis of 2.4 m and a semi-minor axis of 1.7 m, the $\{1,0,0\}$ mode computes to a resonance frequency of 112 Hz, which again agrees well with the measured value of 110 Hz. This may be rather fortuitous, however, given the empirical observation of a second node-antinode pair in the north sub-chamber, and the very irregular pattern in the southeast sub-chamber [see Fig. 4(b) and Jahn *et al.*, 1995].

For a more detailed analysis of this and subsequent sites, we invoked another ad hoc strategy, namely, to partition the structures into sub-chambers having simple three-dimensional geometries. These sub-chambers are not completely closed, but share open surfaces with one another. The particular chamber geometries are selected so that their resulting natural modes are expressible in terms of simple functions. This still leaves open the placement of the partition surfaces and the boundary conditions imposed at those interfaces. Clearly, continuity requires that the acoustic potential and its normal derivative be continuous across the interfaces for all time, which is only possible if the resonance frequencies of the individual sub-chambers agree. We further simplify the problem by imposing an interface boundary condition such as to define modes in the sub-chambers that not only share the same frequency, but also present either a common node on both sides of the interface surface, or a common antinode. This further constraint automatically ensures, respectively, that the acoustic potentials or their normal derivatives are continuous across the interfaces. In this simplified approach we will assume that both continuity conditions are satisfied between pairs of sub-chamber modes that are so constrained, provided they have a similar resonance frequency.

Thus we patch together an elliptical mode in the central chamber with appropriate rectilinear modes in the five sub-chambers, requiring that their phase fronts match smoothly at or near the sub-chamber apertures. Relying on the measurements to exclude modes having angular or vertical variations, the best-matched configuration turns out to require a node to stand near the sub-chamber entrances matching, as it were, a $\{1/2,0,0\}$ elliptical mode in the central chamber to $\{1/2,0,0\}$ rectilinear modes in the northwest (99 Hz), southwest (119 Hz), and southeast (120 Hz) sub-chambers. The matches are not so good with the northeast (67 Hz) and north (58 Hz) sub-chambers. Referring to the experimental map, Fig. 4(b), it appears that the northeast sub-chamber, perhaps because of its trapezoidal shape, pulls the matching node plane well inside its aperture, which would, of course, increase its resonance frequency from the computed value. The north chamber pattern may be complicated by the standing

TABLE II. Resonance frequency at Loughcrew L ancillary chambers.

Chamber	(depth)	$n_x=1/2$	$n_x=3/2$	$n_x=5/2$
NW	(0.87 m)	99	297	495
SW	(0.73 m)	119	355	592
N	(1.50 m)	58	173	290
NE	(1.29 m)	67	199	332
SE	(0.71 m)	120	361	601

stone jutting out from its west wall that may induce the additional antinode at the constriction, disrupting the overall resonance.

Details of these calculations, along with graphs of all radial traverses, are available in Jahn *et al.* (1995); briefly, we apply the method of partitions by choosing surfaces that define each of the ancillary chambers as cuboids. This leaves some freedom in the positioning of the partition planes, and consequently, of the effective dimensions of the central chamber, in acknowledgment of the empirical results. The proposed partition surface corresponds with the measured nodal contour sketched in Fig. 4. Note that the semi-minor axis is approximately the same length as the depth of the northwest and southwest cavities. Because the acoustic potential must have an antinode at the walls, it follows that for a radially symmetric mode with an antinode at the center of the central chamber, we expect nodes in potential to coincide with the partition surfaces. We indicate, by half-integer indices for the radial quantum number, modes which have an antinode at the origin, and a node at the artificial boundary established by the partition surface. The rectilinear results for the modes $\mathbf{m} = \{n_x, 0, 0\}$ in the ancillary chambers are given in Table II. In each case, the mode index n_x corresponds to outward variation of the potential, approximately along a radius from the center of the central chamber. The presence of a possible further partition in the southeast chamber is not considered. The effect of the entrance tunnel is also ignored due to its relatively long length compared to the depths of the ancillary chambers.

For a nodal surface at a constant "elliptical radius" $\xi = \xi_0$, the eigenvalue equation is modified from that of Eq. (3) to

$$Ce_m(\xi_0, q_{m,l}^{(+)}) = 0, \quad Se_m(\xi_0, q_{m,l}^{(-)}) = 0, \quad (9)$$

but the expansion of the acoustic potential [Eq. (2)] is otherwise unchanged. Inserting $a=1.7$ m, $b=0.9$ m into Eq. (4) gives $e=0.83$, $\xi_0=0.62$, whereupon numerical solution of Eq. (9) gives $q_{0,1/2}^{(+)}=2.1$. Computing the resonance frequency from Eq. (5), the first radially symmetric mode with no vertical variation becomes $\{1/2, 0, 0; 114\}$. In Table II we give the resonant frequencies of the ancillary chambers for modes with no vertical or lateral variation corresponding to $\mathbf{m} = \{n_x, 0, 0\}$. We find that three of the ancillary chambers have low-frequency resonances tolerably close both to that computed for the central chamber (114 Hz), and to the measured overall resonance at 110 Hz: NW: $\{1/2, 0, 0; 99\}$, SW: $\{1/2, 0, 0; 119\}$, SE: $\{1/2, 0, 0; 120\}$. For the north and northeast chambers however, there do not exist corresponding natural resonances, and therefore one can expect some departure

TABLE III. Resonance frequencies of Newgrange ancillary chambers bounded by antinodes.

Chamber	(depth)	$n_x=1$	$n_x=2$	$n_x=3$
E	(1.5 m)	115	229	345
N	(2.0 m)	86	172	258
W	(2.9 m)	59	119	178

from the idealized approximation for these two, some hints of which indeed appear on the radial traverses (Jahn *et al.*, 1995). Nonetheless, the relatively good agreement between the resonances for the other chambers and the central ellipse predicts an overall resonance somewhere between 99 Hz and 120 Hz, with modal patterns $\{1/2, 0, 0\}$ for these four chambers, in agreement with measurements.

F. Wayland's Smithy

This cruciform configuration was the first visited, and the acoustical survey was, for several reasons, the least adequate. Measurements were taken for the east and west chambers only, with the source remaining in the central chamber. One might expect these resonances to be compromises between those predicted by the method of partitions for each chamber independently, and the overall resonance for the whole structure. Taking the west chamber to be a cuboid with dimension $1.7 \times 0.7 \times 1.0$ m, and assuming an antinodal surface at the open interface with the central chamber, the resonance frequency of the $\{1, 0, 0\}$ mode is computed to be 102 Hz. For the east chamber, dimensions $1.5 \times 0.8 \times 1.0$ m, treated in a similar fashion, the $\{1, 0, 0\}$ mode computes to 117 Hz. These two are in tolerable agreement with the observed values of 95 and 112 Hz, respectively, and far from the frequencies of the $\{2, 0, 0\}$ modes, which are 205 and 234 Hz, respectively.

G. Newgrange

This cruciform structure also requires the partitioning approach. The natural choice is to represent each of the three arms and the entrance tunnel by cuboids, with the remaining central chamber treated as an ellipsoidal cylinder. Due to the relatively long length of the entrance chamber, the boundary conditions at its entrance will have negligible effect on the modes and resonances frequencies of the structure as a whole. Accordingly, we consider initially just the three arms and the central chamber, whose relative dimensions, as defined by the stone walls, suggest using antinodal surfaces as the artificial boundary conditions at the partition interfaces. Once again, the choice of location of the partition surface, especially with the north chamber pattern, is dictated by the empirical results. Considering modes with no vertical or lateral variation, $\mathbf{m} = \{n_x, 0, 0\}$, the resonance frequencies are listed in Table III.

For the central chamber, consistent with the chosen ancillary dimensions, we take $a=2.0$ m, $b=1.2$ m, giving $e=0.8$, $\xi_0=0.69$, whereupon numerical solution of Eq. (3) gives $q_{0,1}^{(+)}=4.5$. Unfortunately, the first radially symmetric

TABLE IV. Resonance frequencies of Newgrange ancillary chambers bounded by nodes.

Chamber	(depth)	$n_x=1/2$	$n_x=3/2$	$n_x=5/2$
E	(0.8 m)	108	323	538
N	(0.8 m)	108	323	538
W	(2.2 m)	39	117	195

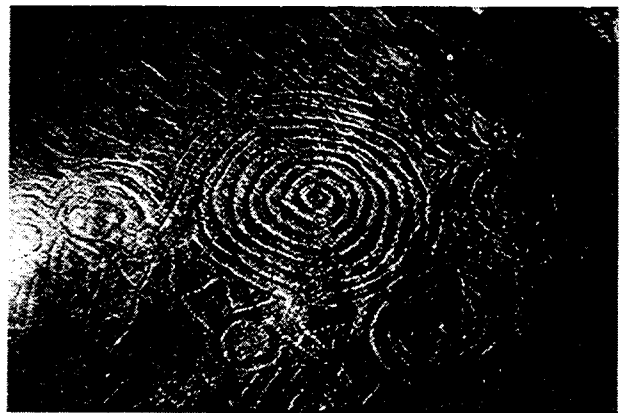


FIG. 7. Rock art—Newgrange interior.

mode with no vertical variation then has a much higher natural frequency than the measured value $\{1,0,0;145\}$, suggesting that the artificial boundaries have been inappropriately placed. We thus must resort to placing the partitions at the next nodal surface, despite the fact that it does not coincide with the apertures defined by the stones closest to the center of the central chamber. Using dimensions derived from the empirical results, if we represent the central chamber as an elliptical cylinder now bounded by a nodal surface, but still taking the ancillary chambers to be cuboids, we find the resonance frequencies for modes with no vertical or lateral variation, $\mathbf{m} = \{n_x, 0, 0\}$, to be those listed in Table IV.

For the central chamber, we now use $a=3.2$ m, $b=2.0$ m, and apply the modified boundary conditions, Eq. (9), numerical solution of which gives $q_{0,1/2}^{(+)}=0.3$ and $q_{0,3/2}^{(+)}=1.1$. The two lowest frequency modes are then $\{1/2,0,0;54\}$ and $\{3/2,0,0;103\}$, suggesting an overall resonance of the latter with the ancillary chamber modes E: $\{1/2,0,0;108\}$, N: $\{1/2,0,0;108\}$, W: $\{3/2,0,0;117\}$. This model agrees far better with the measured resonance at 110 Hz, and with the observed mode structure in the radial traverses.

The long entrance passage presents a fascinating acoustical situation of its own. We would expect that sound waves driven into the passage from the central chamber should propagate, with some attenuation, along the full length, and partially reflect from the exit orifice to establish a decaying longitudinal standing-wave pattern throughout. Since the cross section of the tunnel is of the order of 1 m wide \times 2 m high over most of its length, and since the free space wavelength associated with 110 Hz is about 3.13 m, no modes other than $\{n_x, 0, 0\}$ are likely to appear. For the former, the predicted nodal spacing is simply one-half the free-space wavelength, or about 1.5 m, which is essentially that observed. Over the 17 m from the first node in the hall to the exit this computes to 10.87 node-to-node transitions compared to the roughly 10.5 observed [Fig. 6(d)]. Note that this corresponds to approximately 12 antinode-to-antinode transitions from the center of the main chamber to the exit, which also agrees with measurements. The anticipated attenuation outward along the passage is also confirmed, with a slight recovery of amplitude as the pattern passes under the large entrance capstone.

III. ROCK ART

The Newgrange and Loughcrew sites present extraordinary and well-known examples of diagrammatic rock etchings conventionally regarded as astronomical, seasonal, or environmental representations (O'Kelly, 1993; Thomas,

1988). In several cases, however, the experimenters were struck by the similarities of several of these to the resonant sound patterns characterizing the chambers. For example, a number of these sketches feature concentric circles, ellipses, or spirals that are not unlike the plan views of the acoustical mappings (see Fig. 7). In others, sinusoidal or zigzag patterns resemble the alternating nodes and antinodes found in the radial traverses. For example, the two zigzag trains etched on the corbel at the left side of the west sub-chamber of Newgrange have precisely the same number of "nodes" and "antinodes" as the resonant standing-wave pattern we mapped from the chamber center cut along the passage. Similarly, one of the Kerbstones displays a triple zigzag above a spot and two concentric circles, which in number and spacing resemble the modal patterns radiating from the central chamber into the recesses. Conceivably, the triple spiral configurations sketched on the magnificent entrance stone and elsewhere could also be somewhat more metaphysical representations of the interactive resonances of the three sub-chambers.

IV. SUMMARY

The experimental data and theoretical analyses presented above constitute little more than a pilot study addressing the hypothesis that these ancient structures possessed resonant acoustical properties that may have contributed to their functional purposes. The extent to which these features were deliberately engineered into these sites, and their particular utilization, are beyond the scope of this study, but certain suggestive aspects, perhaps worthy of more extensive and precise surveys, have been noted. First, by whatever course of design and construction, all six of the diverse configurations visited sustain clearly discernible acoustical resonances in the vicinity of 110 Hz, well within the male voice range. The dominant standing-wave patterns at these frequencies are the principle radial or longitudinal harmonics, with little azimuthal or vertical variation. In a few cases, it appears that interior standing stones may have been positioned to enhance such resonances, by suppressing unwanted azimuthal modes. At some sites, a number of the rock art

drawings bear striking similarities to the plan or longitudinal patterns of these standing-wave configurations.

Further pursuit of this hypothesis will require much more detailed and precise mapping of these or similar sites, and extension of the techniques to other locales and eras, to establish the breadth and endurance of such acoustical characteristics. It would also be instructive to search the existing reservoirs of archeological and anthropological understanding for evidence of ancient cultural attention to other acoustical phenomena.

ACKNOWLEDGMENTS

The authors are indebted to those agencies in the British Isles who provided access to, and information about, the various sites studied, most notably the National Monuments

Branch of the Office of Public Works, Ireland, for special arrangements with respect to Newgrange. We also appreciate the assistance of Mr. John Bradish in designing and assembling the field equipment, and of Ms. Charla Devereux and Ms. Brenda Dunne in performing the field experiments. This work was supported by a grant from the Fetzer Institute.

- Abramowitz, M., and Stegun, I. (1970). *Handbook of Mathematical Functions* (Dover, New York).
- Jahn, R. G., Devereux, P., and Ibison, M. (1995). *Acoustical Resonances of Assorted Ancient Structures*, PEAR Technical Report No. 95002 (Princeton University, Princeton).
- McLachlan, N. W. (1964). *Theory and Application of Mathieu Functions* (Dover, New York).
- O'Kelly, C. (1993). *Concise Guide to Newgrange* (O'Kelly, Cork, Ireland).
- Schiff, L. I. (1968). *Quantum Mechanics* (McGraw-Hill, Tokyo).
- Thomas, N. L. (1988). *Irish Symbols of 3500 BC* (Mercier, Dublin).